A High Efficiency HPF-ZCS-PWM Sepic for Electronic Ballast With Multiple Tubular Fluorescent Lamps

Fabio Toshiaki Wakabayashi

Carlos Alberto Canesin

Paulista State University
UNESP – FEIS – DEE
LEP – Power Electronics Laboratory
P.O. Box 31 – 15385-000
Ilha Solteira (SP) – Brazil
Fax: +55 (18) 3742-2735

Abstract: **This paper presents a high efficiency Sepic rectifier for an electronic ballast application with multiple fluorescent lamps. The proposed Sepic rectifier is based on a Zero-Current-Switching (ZCS) Pulse-Width-Modulated (PWM) soft-commutation cell. The high power-factor of this structure is obtained using the instantaneous average-current control technique, in order to attend properly IEC61000-3-2 standards.**

The inverting stage of this new electronic ballast is a classical Zero-Voltage-Switching (ZVS) Half-Bridge inverter.

A proper design methodology is developed for this new electronic ballast, and a design example is presented for an application with five fluorescent lamps 40W-T12 (200W output power), 220V_{rms} input voltage, 130V_{dc} dc link voltage, with rectifier and inverter stages operating at 50kHz.

Experimental results are also presented. The THD at input current is equal to 6.41%, for an input voltage THD equal to 2.14%, and the measured overall efficiency is about 92.8%, at rated load.

I. INTRODUCTION

In the last years, electronic ballasts have been implemented in order to overcome some drawbacks of conventional electromagnetic ballasts, namely: significant size and weight, presence of stroboscopic effect, audible noise, and low efficiency.

Usually, electronic ballasts present a rectifying stage followed up by a high frequency inverting stage. This high operating frequency can provide conditions to reduce the size and weight of the required reactive devices (capacitors and inductors), and, in addition, the stroboscopic effect and the audible noise can be suppressed. Moreover, when fluorescent lamps are fed up with high frequency currents, their luminous efficiency (lumens/Watts) can be increased when compared to fluorescent lamps operating at low frequencies [1].

In order to improve even more the electronic ballasts, rectifying stages with power factor correction techniques have been analyzed in several papers [2-4].

However, operating semiconductor devices at high frequencies can cause significant commutation losses. In this way, new rectifying and inverting stages, which incorporate soft-commutation techniques, have been proposed.

Finally, in order to reduce inherent costs of electronic ballasts, improving the attractiveness of these lighting systems, the concept of electronic ballasts applied to multiple fluorescent lamps has been developed [4].

According to this context, this paper presents a new high-power-factor electronic ballast applied to a set of five tubular fluorescent lamps (40W-T12). The input stage of this ballast is a zero-current-switching (ZCS) pulse-width-modulated (PWM) Sepic rectifier, controlled by the instantaneous average current technique. Its output stage is a classical zero-voltage-switching (ZVS) Half-Bridge inverter, controlled by a low cost IC (IR2155).

II. THE NEW HPF ELECTRONIC BALLAST

The new electronic ballast is shown in Fig. 1. According to this figure, it can be seen that the rectifying stage presents a ZC commutation cell, derived from [5, 6], with two active switches (S_1 and S_2), two diodes (D_1 and D_2), two small resonant inductors (L_{r1} and L_{r2}), and one resonant capacitor (C_r).

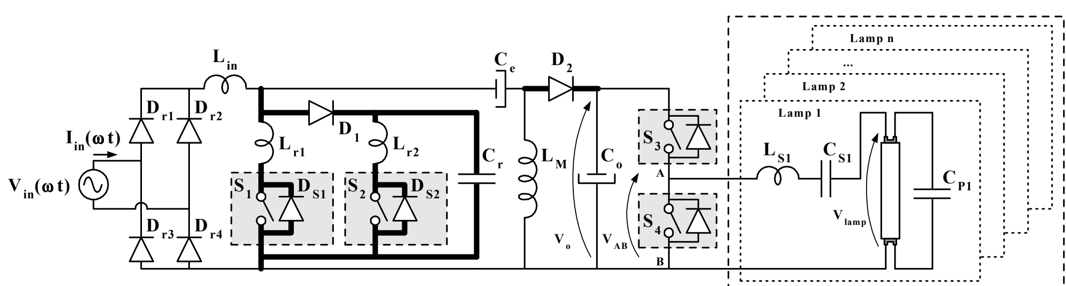

Figure 1 – New high efficiency Sepic rectifier applied at an electronic ballast for multiple tubular fluorescent lamps.

The main advantage of this commutation cell, when compared to that one presented in [6], is the position of D_1: in the non-isolated application proposed in this paper, S_1 and S_2 present one single reference point to their gate drives. Furthermore, diodes D_1 and D_2 are not associated in a series connection in any operating stage, preserving the main characteristics of the cell presented in [6].

Regarding to the inverting stage, it can be verified that it is a Half-Bridge converter connected to asymmetrical voltage fed resonant filters (L_{sn}, C_{sn}, and C_{pn}).

III. Theoretical Analysis

III.A. New HPF-ZCS-PWM Sepic Rectifier

The analysis of this Sepic rectifier can be simplified, maintaining a satisfactory accuracy, if the following conditions are assumed:

- all components are ideal;
- the switching frequency (f_{Sepic}) is much higher than the ac line frequency (f_{line}), so the input voltage can be considered practically constant during one switching period (T_{Sepic});
- the input filter (L_{in}) associated with the input rectifier (D_{r1} until D_{r4}) are replaced by an input rectified current source ($|I_{in}(\omega t)|$), and it is assumed constant ($|I_{in}(\omega T_i)|$) during a generic Sepic switching period ($T_i=T_{Sepic}$);
- the accumulation inductance (L_M) is large enough to be considered as a constant current source ($I_M=I_{o(nom)}$, where $I_{o(nom)}$ is the nominal value of the output current);
- the accumulation capacitance (C_e) is replaced by a constant voltage source ($V_{Ce}(\omega t)=|V_{in}(\omega t)|$, where $V_{in}(\omega t)$ is the instantaneous value of the input voltage), during a generic Sepic switching period (T_i);
- the output voltage (V_o) is constant.

III.A.1. Topological Stages

The main ideal waveforms and topological stages of this proposed rectifier, during a generic Sepic switching period, are presented in Fig. 2. From this figure, it can be verified that the main switch S_1 is turned on at $\omega t=\omega t_0$, and the auxiliary switch S_2 at $\omega t=\omega t_2$, both at zero-current (ZC). Furthermore, S_1 and S_2 are turned off simultaneously, in the sixth stage ($\Delta t_6=\omega t_6-\omega t_5$), at zero-current and zero-voltage (ZCZV). Diodes D_1 and D_2 present zero-voltage (ZV) turn-on processes, at $\omega t=\omega t_3$ and $\omega t=\omega t_8$, respectively.

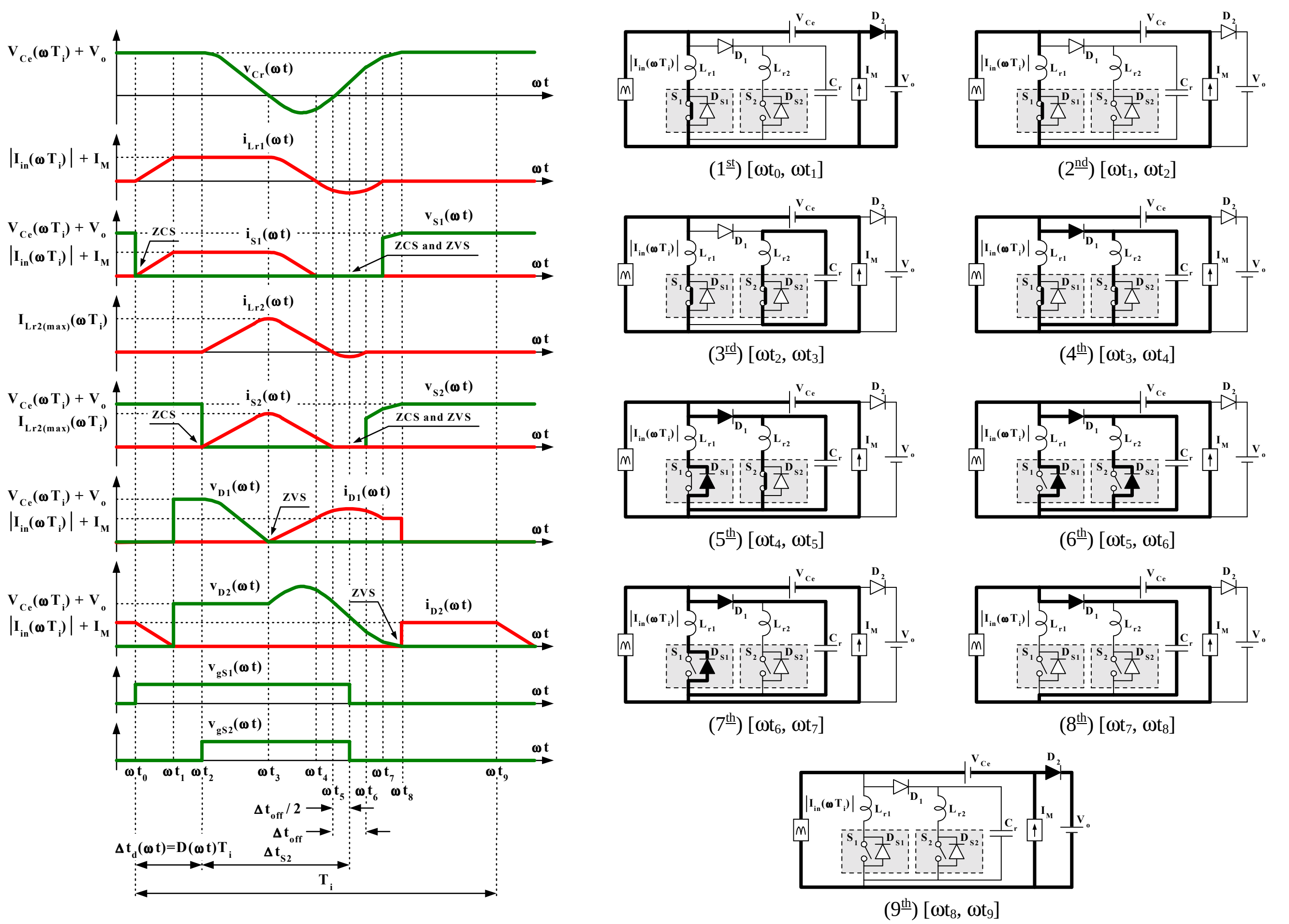

(a) (b)

Figure 2 – (a) Main ideal waveforms; and (b) Topological stages for the HPF ZCS-PWM Sepic rectifier, during a generic Sepic switching period (T_i).

III.A.2. Analysis of Commutation

The analysis of this Sepic rectifier is similar to the analysis presented in [6], for its isolated version. So, in the following, the main constraints and relevant equations are summarized:

$$\beta = \frac{L_{r2}}{L_{r1}} < 1; \tag{1}$$

$$\alpha_{max} = \frac{I_o}{V_o}\sqrt{\frac{L_{r2}}{C_r}} < \beta; \tag{2}$$

$$\Delta t_{off} = \Delta t_6 = \frac{2}{\omega_{02}}\left(\frac{\pi - a\cos(-\beta)}{\sqrt{1+\beta}}\right); \tag{3}$$

$$\Delta t_{S2} = \frac{1}{\omega_{02}}\left[\frac{\pi}{2} + \frac{\pi}{\sqrt{1+\beta}}\right]; \tag{4}$$

where:

$$\omega_{02} = \frac{1}{\sqrt{L_{r2}C_r}}. \tag{5}$$

As commented in [5, 6], values of β near to the unity leads to significant volume for the resonant inductors, and very low values of *f* are responsible for high resonance frequencies, increasing magnetic losses and problems of electromagnetic interference. In this way, it is necessary to choose values for β and *f* that will provide conditions to obtain a weak influence from resonance over the output regulation, and will also avoid the problems of increasing volume, magnetic losses, and electromagnetic interferences.

III.B. Resonant Half-Bridge Inverter

III.B.1. Topological Stages

Fig. 3 shows the four topological stages and main ideal waveforms, from one operating period of the resonant Half-Bridge inverter. S_3 and S_4 are complementary operated.

It is necessary to take into account that, in the resonant Half-Bridge inverter, the active switches will perform ZV turn-on processes if the Half-Bridge switching frequency (f_{HB}) is higher than the resonant frequency from the series branch (f_{SB}), where:

$$f_{SB} = \frac{1}{2\pi\sqrt{L_s C_s}}; \tag{6}$$

and:

$$L_s = L_{s1} = L_{s2} = \ldots = L_{sn};$$

$$C_s = C_{s1} = C_{s2} = \ldots = C_{sn}.$$

The characteristic of a fluorescent lamp operating at high frequencies is similar to a resistive load [7]. So, in order to simplify the analysis of this circuit, the lamp connected to the output of this inverting stage is replaced by an equivalent resistance (R_{lamp}).

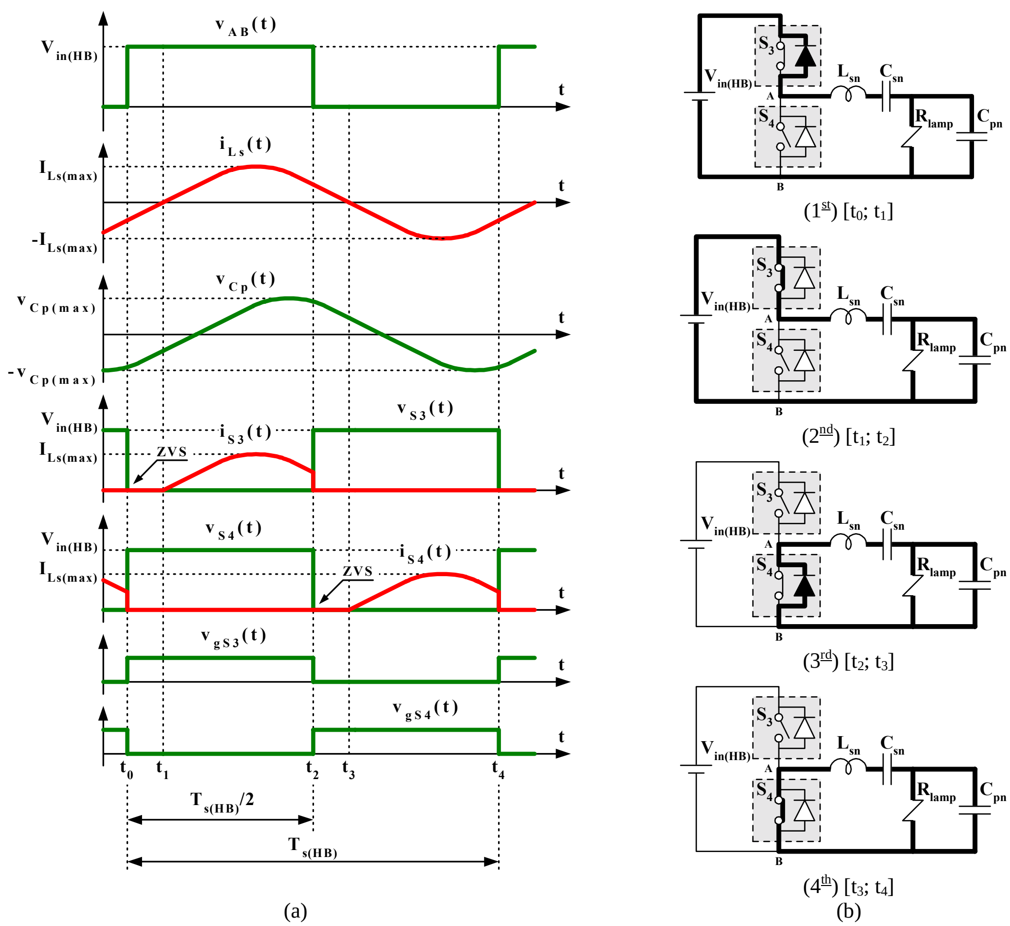

Figure 3 – (a) Main ideal waveforms; and (b) Topological stages for the resonant Half-Bridge inverter, during one Half-Bridge switching period ($T_{s(HB)}$).

III.B.2. Lamp Ignition Process

In the lamp ignition process, it is necessary to ensure the preheating process, in order to avoid damages in the lamp electrodes. After it, a proper ignition voltage must be applied across the lamp for the development of the first arc. As mentioned in [6], the obtaining of high voltage values across the lamp can be achieved by setting up the switching frequency of inverting stage (f_{HB}) equal to, or near to, the resonant frequency during ignition (fr), where:

$$f_r = \frac{1}{2\pi\sqrt{L_s \frac{C_s C_p}{C_s + C_p}}}; \qquad (7)$$

and: $$C_p = C_{p1} = C_{p2} = \ldots = C_{pn}.$$

The theoretical waveforms of the voltage over the lamp are shown in Fig. 4, for different values of f_{HB}.

When $f_{HB} \neq f_r$ it can be seen that the peak value of the voltage over the lamp can be limited, avoiding damages in the circuit components if the ignition process fails.

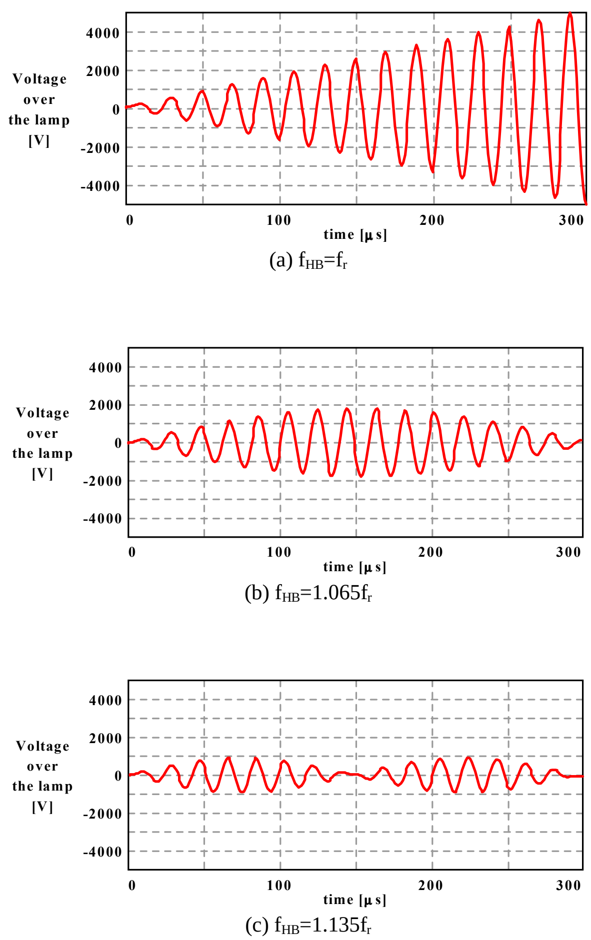

(a) $f_{HB}=f_r$

(b) $f_{HB}=1.065f_r$

(c) $f_{HB}=1.135f_r$

Figure 4 – Theoretical voltage waveform over the lamp, during ignition process.

Also, according to the analysis presented in [6], the higher the difference between f_{HB} and f_r, the lower will be the peak value of the voltage over the lamp. This fact implies in the possibility of slowing down the obtaining of high peak values of voltage, providing conditions to the evolution of the preheating process. The desired Half-Bridge switching frequency variation can be obtained using the parallel capacitor switching technique [8].

IV. Design Example

The new electronic ballast is designed according to the input and output data presented in Table I.

The rectifying stage is designed according to the procedure presented in [6]. The following parameters are adopted:

$$\beta = 0.43, f = 0.10, \text{ and } \alpha_{max} = 0.342.$$

So, the resonant devices are:

$$C_r = 11nF, L_{r1} = 21.4\mu H, \text{ and } L_{r2} = 9.2\mu H.$$

From the procedure proposed in [5], the input filter is:

$$L_{in} = 5mH.$$

The accumulation inductance (L_M) must provide a ripple lower than 20% at its current. The accumulation capacitance (C_e) is obtained from a trade-off between the need of low high frequency voltage ripple and low input current THD. So, were specified:

$$L_M = 2mH, \text{ and } C_e = 330nF.$$

Finally, the output filter (C_o) is designed for a ripple restricted to no more than to 2% of V_o nominal value:

$$C_o = 1360\mu F.$$

Details for designing a classical resonant Half-Bridge inverter are presented in [6]. However, the following equations are more accurate for designing the required resonant devices:

$$f_{ign} = \frac{f_{HB}}{f_r} > 1; \qquad (8)$$

TABLE I

Input and Output Data

Input voltage	$220V_{rms} \pm 15\%$
Line frequency	60Hz
Sepic switching frequency	50kHz
Dc link voltage ($V_{o(nominal)}$)	$130V_{dc}$
Nominal Half-Bridge switching frequency	50kHz
Lamp voltage ($V_{lamp(rms)}$)	$120V_{rms}$
Preheating frequency	85kHz
Minimum pre-heating time interval	200ms
Lamp ignition voltage	$500V_{pk-pk}$
Minimum input stage efficiency	95%
Nominal Output power (five 40W-T12 fluorescent lamps)	200W

$$f_{zvs} = \frac{f_{HB}}{f_{SB}} > \sqrt{\frac{f_{ign} V_{AB(rms)}}{V_{AB(rms)} + (1 - f_{ign}^2) V_{lamp(rms)}}} ; \quad (9)$$

$$C_s = F \frac{P_{lamp}}{V_{AB(rms)} V_{lamp(rms)}} ; \quad (10)$$

$$L_s = \frac{f_{zvs}^2}{(2\pi f_{HB})^2 C_s} ; \quad (11)$$

$$C_p = \frac{f_{ign}^2}{f_{zvs}^2 - f_{ign}^2} Cs ; \quad (12)$$

$$F = \frac{1 - f_{zvs}^2}{2\pi f_{HB} \sqrt{1 - \left[\frac{f_{zvs}^2 (1 - f_{ign}^2)}{(f_{zvs}^2 - f_{ign}^2)} \frac{V_{lamp(rms)}}{V_{AB(rms)}} \right]^2}} . \quad (13)$$

where:

$V_{AB(rms)}$ = rms value of voltage over the resonant tank.

Then, adopting: $f_{ign} = 1.075$;

$f_{zvs} = 4$;

the resonant devices of the Half-Bridge inverter are obtained:

$C_s = C_{s1}$ until C_{s5} = 330nF,

$L_s = L_{s1}$ until L_{s5} = 500µH, and

$C_p = C_{p1}$ until C_{p5} = 22nF.

V. Experimental Results

The main results obtained from an implemented prototype for the new electronic ballast are presented in the following figures. The input current of the rectifier, at nominal input voltage and full load is shown in Fig. 5, as well as its frequency spectrum. The measured input current THD is equal to 6.41%, when the input voltage THD is equal to 2.14%. Its measured power factor is almost the unity (0.995).

These results can be verified observing that the waveform of the input current is very similar to the waveform of the input voltage. In addition, the phase displacement between input current and input voltage is negligible, attending all requirements from IEC61000-3-2 standards.

The commutation details for the active switches of the Sepic rectifier are shown in Figs. 6 and 7, obtained when the instantaneous input voltage was near to zero ($V_{in}(\omega t) \cong 0$), and when it was near to its peak value ($V_{in}(\omega t) \cong V_{in(pk)}$).

From the analysis of Figs. 6 and 7, it is possible to note that both switches perform ZC turn-on processes, and ZCZV turn-off processes. Moreover, it can be observed that these commutations are preserved during an ac system period, minimizing the commutation losses associated to these devices, and implying in a high efficiency for this stage.

Fig. 8 shows the current through D_1 and D_2, during one generic switching period. In this figure, it is possible to note that they do not present a series connection, during any operating stage.

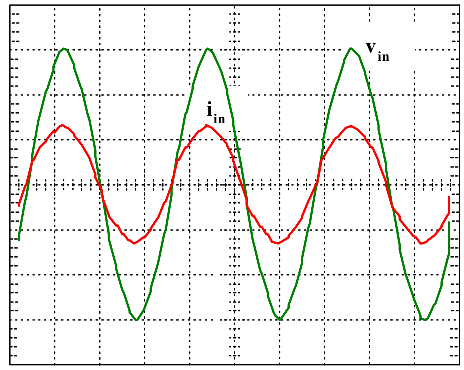

(a) V_{in}: 100V/div, 5ms/div ; I_{in}: 1A/div; 5ms/div

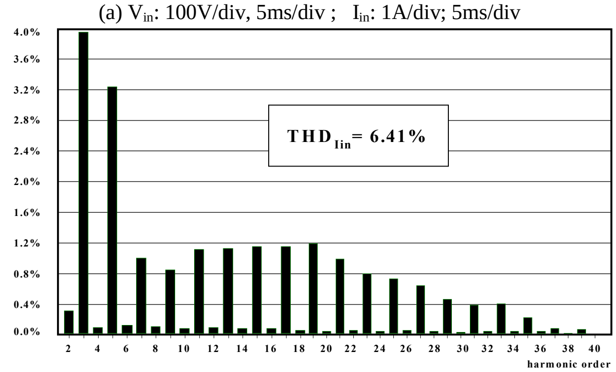

(b)

Figure 5 – (a) Input voltage and input current, and (b) frequency spectrum of I_{in}, at rated load.

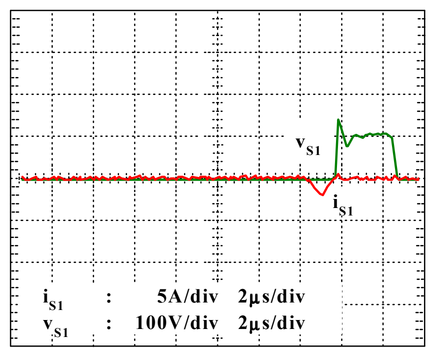

(a) $V_{in}(\omega t) \cong 0$

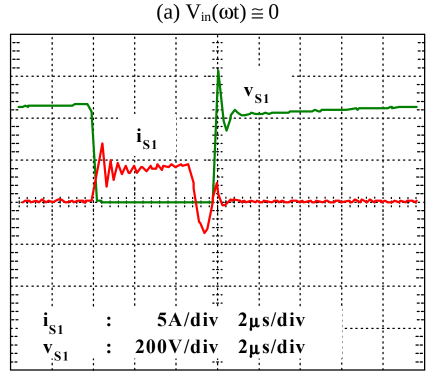

(b) $V_{in}(\omega t) \cong V_{in(pk)}$

Fig. 6 – Commutation details in the new HPF-ZCS-PWM Sepic rectifier, for main switch, at full load: (a) near to $V_{in}(t)=0$, (b) near to $V_{in}(t)=V_{in(pk)}$.

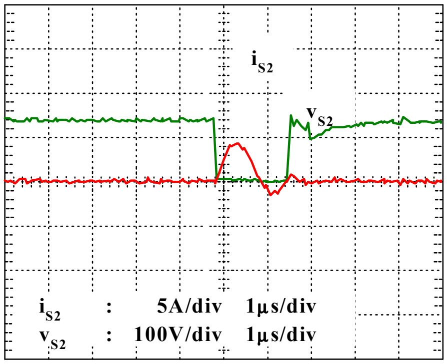

(a) $V_{in}(\omega t) \cong 0$

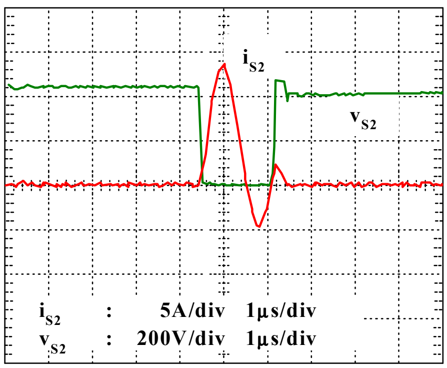

(b) $V_{in}(\omega t) \cong V_{in(pk)}$

Fig. 7 – Commutation details in the new HPF-ZCS-PWM Sepic rectifier, for auxiliary switch, at full load: (a) near to $V_{in}(t)=0$, (b) near to $V_{in}(t)=V_{in(pk)}$;

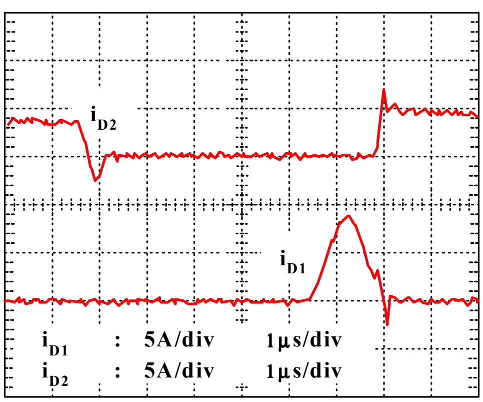

Fig. 8 – Currents through D_1 and D_2, respectively.

The commutation details of the switches employed in the Half-Bridge inverter are shown in Fig. 9, where it can be seen that both semiconductors presents a ZV turn-on process.

The overall efficiency measured in this prototype is equal to 92.8%, at full load.

After ignition, the voltage over the lamp and the current across L_{s1} assume the waveforms shown in Fig. 10. The measured crest factor of the current acroos the lamp is equal to 1.44.

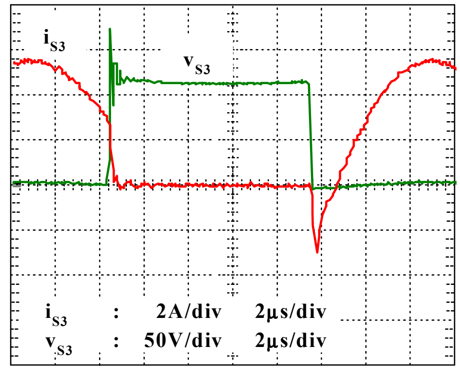

(a)

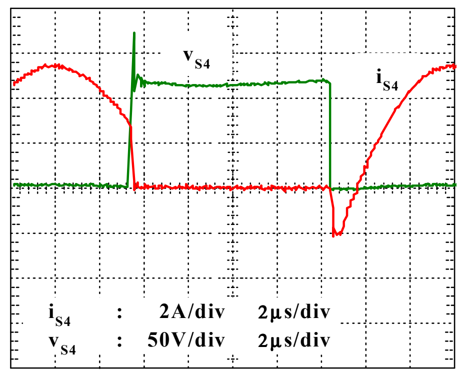

(b)

Figure 9 – Commutation details in the Half-Bridge inverter, at full load: (a) switch S_3, and (b) switch S_4.

The ignition process, including the preheating process and the obtaining of high peak values of voltage over the lamp, is shown in Fig. 11. According to this figure, the preheating time interval is about 250ms. For obtaining this preheating process, the control of the inverter stage was implemented following the steps described in [6]. It can be seen that the voltage evolves through two stages, until it reaches the required value to provide the lamp ignition (in this case, near to $500V_{pk-pk}$).

Finally, one detail of the limit imposed to the evolution of the voltage over the lamp is shown in Fig. 12.

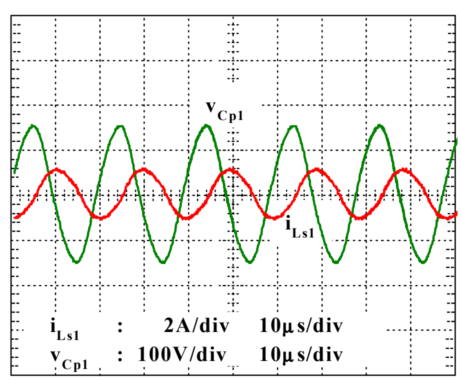

Figure 10 – Voltage and current across one of five fluorescent lamps.

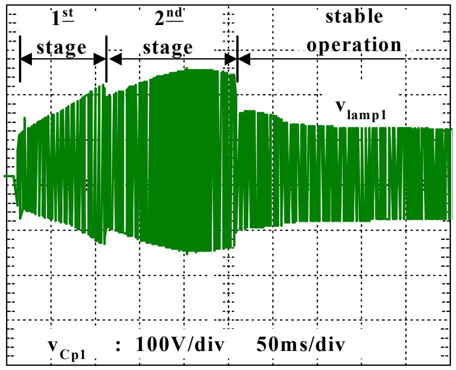

Figure 11 – Lamp ignition process.

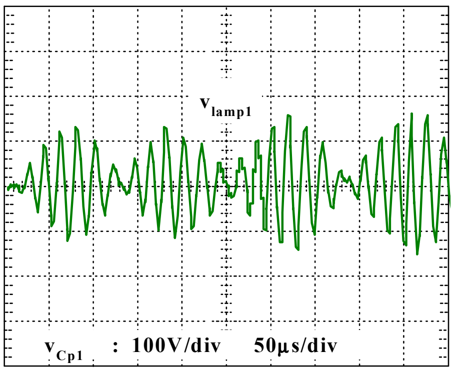

Figure 12 – Limit imposed to the peak value of the voltage over the lamp.

VI. Conclusions

This paper presented a new electronic ballast for multiple tubular fluorescent lamps, employing a high-efficiency Sepic rectifier as a high power-factor input stage.

The active switches of this Sepic rectifier perform ZC commutations during their turn-on processes, and ZCZV commutations during their turn-off processes. Also, D_1 and D_2 present ZV commutations during their turn-on processes, and their reverse recovery effects over actives switches are minimized.

This new arrangement for the soft-commutation cell provides a single reference point to the active switches, simplifying the control circuitry, when compared to that one required to the commutation cell presented in [6].

The input current of this new electronic ballast presented low THD (6,41%) and low phase displacement, due to the average-current mode control employed in this preregulator stage, resulting in a power factor near to the unity, and attending IEC 61000-3-2 standards.

In the resonant Half-Bridge inverter, the active switches performed ZV turn-on process, as expected. Also, the obtaining of a desired preheating time interval and the limitation of the maximum voltage across the lamp during the ignition process was possible, using a proper design procedure and a low cost IC (IR2155).

Finally, the measured overall efficiency of this new electronic ballast is equal to 92.8, at full load.

Acknowledgments

The authors would like to thanks to FAPESP for supporting this work.

References

[1] M. S. Rea, “The IESNA Lighting Handbook – Reference and Application”, Illuminating Engineering Society of North America, in CD-ROM.

[2] J. Spangler, B. Hussain, and A. K. Behera, “Electronic Fluorescent Ballast Using a Power Factor Correction Techniques for loads Greater Than 300 Watts”, in Proc. IEEE APEC Rec., 1991, pp. 393-399.

[3] M. A. Có, D. S. L. Simonetti, and J. L. F. Vieira, “High-Power-Factor Electronic Ballast operating in Critical Conduction Mode”, IEEE Transactions on Power Electronics, vol. 13, no. 1, January 1998, pp. 93-101.

[4] R. Gules, E. U. Simões, and I. Barbi, “A 1.2kW Electronic Ballast for Multiple Lamps, with Dimming Capability and High-Power-Factor”, in Proc. IEEE APEC Rec., 1999, pp. 720-726.

[5] M. J. Bonato, F. T. Wakabayashi and C. A. Canesin, “A Novel Voltage Step-Down/Up ZCS-PWM Zeta Converter”, in Proc. IEEE IAS Annual Meeting Rec., 2000, in CD-ROM.

[6] F. T. Wakabayashi, and C. A. Canesin, “Novel High-Power-Factor isolated Electronic Ballast for Multiple Tubular Fluorescent Lamps”, in Proc. IEEE IAS Annual Meeting Rec., 2001, in CD-ROM.

[7] E. E. Hammer, “High Frequency Characteristics of Fluorescent Lamps up to 500kHz”, in Journal of IES, Winter 1987, pp. 52-61.

[8] J. Parry, “Variable Frequency Drive using IR215X Self-Oscillating IC’s”, in Lighting Ballast Control IC – Designer’s Manual 2001, International Rectifier, pp. 331.